Published in *Phys. Fluids* **14**, L73-L76 (2002).

Contribution of Reynolds stress distribution to the skin friction in wall-bounded flows

Koji Fukagata *, Kaoru Iwamoto, and Nobuhide Kasagi

Department of Mechanical Engineering, The University of Tokyo,
7-3-1 Hongo, Bunkyo-ku, Tokyo 113-8656, Japan

(Dated: 1 October 2002)

A simple expression is derived of the componential contributions that different dynamical effects make to the frictional drag in turbulent channel, pipe and plane boundary layer flows. The local skin friction can be decomposed into four parts, i.e., laminar, turbulent, inhomogeneous and transient components, the second of which is a weighted integral of the Reynolds stress distribution. It is reconfirmed that the near-wall Reynolds stress is primarily important for the prediction and control of wall turbulence. As an example, the derived expression is used for an analysis of the drag modification by the opposition control and by the uniform wall blowing/suction.

The frictional drag of a turbulent wall-bounded flow is usually much higher than that of a laminar one. Owing to extensive research over the last several decades, we presently have a common understanding that such large frictional drag is attributed to the existence of near-wall vortical structure and the associated ejection/sweep events [1].

This important knowledge results in, for instance, dynamical argument-based control algorithms for drag reduction in wall-bounded turbulent flows. Choi *et al.* [2] demonstrated in their direct numerical simulation (DNS) that about 25 % drag reduction can be attained by a simple algorithm, in which local blowing/suction is applied at the wall so as to oppose the wall-normal velocity at 10 wall units above the wall. Later on, different control algorithms for drag reduction have been tested with DNS and the drag reduction mechanism has been discussed based on the statistics of the controlled flow and also the visualized turbulence structures[2–5].

However, the quantitative relation between the statistical information of the flow and the drag reduction effect seems to remain not completely clear. In the present Letter, we derive a direct relation between the skin friction coefficient and the Reynolds stress distribution for three canonical wall-bounded flows, i.e., channel, pipe and plane boundary layer flows. Although the derivation itself is simple and straightforward, the result is suggestive and useful for analyzing the effect of the Reynolds stress on the frictional drag, especially for controlled flows.

First, we define several dimensionless quantities and averaging operators used. The Reynolds averaged Navier-Stokes equation in the x direction for an incompressible plane channel flow shown in Fig. 1a is given by

$$-\overline{\frac{\partial p}{\partial x}} = \frac{\partial}{\partial y}\left[\overline{u'v'} - \frac{1}{Re_b}\frac{\partial \overline{u}}{\partial y}\right] + \overline{I_x} + \frac{\partial \overline{u}}{\partial t} \; . \tag{1}$$

Here, the overbar of $\overline{f}$ denotes an average of a quantity f in the homogeneous (z) direction, i.e.,

$$f(x,y,z,t) = \overline{f}(x,y,t) + f'(x,y,z,t) \; . \tag{2}$$

* Corresponding author. Also at: Institute for Energy Utilization, AIST, 1-2-1 Namiki, Tsukuba-shi, Ibaraki 305-8564, Japan. E-mail: fukagata@thtlab.t.u-tokyo.ac.jp

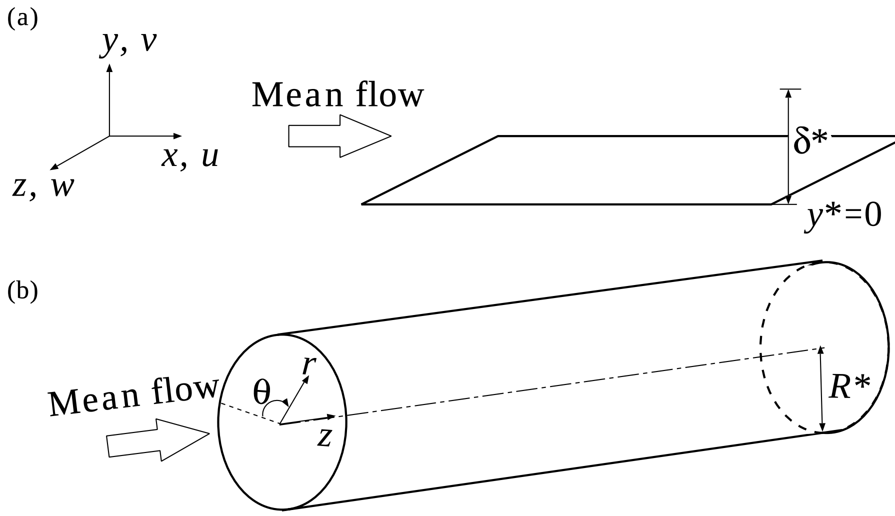

FIG. 1: Flow geometry. (a) channel (half) and plane boundary layer; (b) pipe.

Hereafter, all variables without superscript are those nondimensionalized by the channel half width, δ^*, and twice the bulk mean velocity, $2U_b^*$, whereas dimensional variables are denoted by the superscript of $*$. The bulk Reynolds number is defined as

$$Re_b = \frac{2U_b^*\delta^*}{\nu^*}\ , \tag{3}$$

where ν^* is the kinematic viscosity. The pressure in Eq. (1) is normalized by the density, and $\overline{I_x}$ contains the terms appearing when the flow is inhomogeneous in the streamwise direction, i.e.,

$$\overline{I_x} = \frac{\partial\overline{(uu)}}{\partial x} + \frac{\partial(\overline{u}\,\overline{v})}{\partial y} - \frac{1}{Re_b}\frac{\partial^2\overline{u}}{\partial x^2}\ . \tag{4}$$

Presently, the following conditions are assumed:

(A) constant flow rate,
(B) homogeneity in the spanwise (z) direction,
(C) symmetry with respect to the center plane,
(D) $u = w = 0$ (i.e., no-slip streamwise/spanwise velocity) on the wall.

It is worth noting that no restriction is made for the wall-normal velocity at the wall. From conditions (A) and (C), its mean should be zero ($\overline{v}(x,0,z,t) = 0$), while its fluctuating part is not necessarily zero ($v'(x,0,z,t) \neq 0$). This enables use of the relation derived below to, for instance, a flow controlled by blowing/suction with zero net flux, that is exemplified later.

Under the conditions above, integration of Eq. (1) over y gives the relation between the pressure gradient and the skin friction coefficient, i.e.,

$$-\frac{\widetilde{\overline{\partial p}}}{\partial x} = \frac{1}{8}C_f(x,t) + \widetilde{\overline{I_x}}\ , \tag{5}$$

where $\widetilde{\overline{f}}$ is the local bulk mean quantity, i.e.,

$$\widetilde{\overline{f}}(x,t) = \int_0^1 \overline{f}(x,y,t)dy \, , \tag{6}$$

and the local skin friction coefficient is defined as

$$C_f(x,t) = \frac{\overline{\tau_w^*}}{\frac{1}{2}\rho^* U_b^{*2}} = \frac{8}{Re_b} \left. \frac{d\overline{u}}{dy} \right|_{y=0} \, , \tag{7}$$

Substitution of Eq. (5) into Eq. (1) results in

$$\frac{1}{8}C_f = \frac{\partial}{\partial y}\left[\overline{u'v'} - \frac{1}{Re_b}\frac{\partial \overline{u}}{\partial y}\right] + I_x'' + \frac{\partial p''}{\partial x} + \frac{\partial \overline{u}}{\partial t} \, , \tag{8}$$

where

$$f''(x,y,t) = \overline{f}(x,y,t) - \widetilde{\overline{f}}(x,t) \, . \tag{9}$$

The relation for componential contributions of different dynamical effects to the local skin friction coefficient can be obtained by applying triple integration, i.e., $\int_0^1 dy \int_0^y dy \int_0^y dy$, to Eq. (8). The first integration essentially gives the force balance, similar to the well-known linear relation for stresses. The second is an integration that leads to the mean velocity profile. The third is akin to obtaining the flow rate from the velocity profile. By using the definition of the the bulk mean velocity, i.e., $\widetilde{\overline{u}} = \int_0^1 \overline{u} \, dy = 1/2$, and by transforming multiple integrations to single integrations by applying the integration by parts, it results in

$$\begin{aligned} \frac{1}{2} \;=\; & Re_b \left[\frac{C_f}{24} - \int_0^1 (1-y)(-\overline{u'v'}) \, dy \right. \\ & \left. + \frac{1}{2}\int_0^1 (1-y)^2 \left(I_x'' + \frac{\partial p''}{\partial x} + \frac{\partial \overline{u}}{\partial t} \right) dy \right] \, . \end{aligned} \tag{10}$$

or, equivalently, by isolating C_f we obtain

$$\begin{aligned} C_f = \; & \frac{12}{Re_b} + 12\int_0^1 2(1-y)(-\overline{u'v'}) \, dy \\ & -12\int_0^1 (1-y)^2 \left(I_x'' + \frac{\partial p''}{\partial x} + \frac{\partial \overline{u}}{\partial t} \right) dy \, . \end{aligned} \tag{11}$$

This equation indicates that the skin friction coefficient is decomposed into the laminar contribution, $12/Re_b$, which is identical to the well-known laminar solution, the turbulent contribution (the second term), and the inhomogeneous and transient contribution (the third term). The turbulent contribution is proportional to the weighted average of Reynolds stress, of which weight linearly decreases with the distance from the wall. This fact quantitatively supports the observation in turbulent channel flow[6] that the turbulence structure that appear closer to the wall than the position of maximum Reynolds stress is most responsible for the frictional drag in wall turbulence.

A similar relationship can be derived also in the case of cylindrical pipe flow, shown in Fig. 1b, by starting from the longitudinal momentum equation in the cylindrical coordinates, i.e.,

$$-\overline{\frac{\partial p}{\partial z}} = \frac{1}{r}\frac{\partial}{\partial r} r \left[\overline{u_r' u_z'} - \frac{1}{Re_b}\frac{\partial \overline{u_z}}{\partial r}\right] + \overline{I_z} + \frac{\partial \overline{u_z}}{\partial t} \, , \tag{12}$$

where

$$\overline{I_z} = \frac{1}{r}\frac{\partial(r\overline{u_r}\,\overline{u_z})}{\partial r} + \frac{\partial\overline{(u_z u_z)}}{\partial z} - \frac{1}{Re_b}\frac{\partial^2\overline{u_z}}{\partial z^2}\ . \tag{13}$$

The definitions of dimensionless quantities are similar as those for channel flow, e.g., in Eq. (3), δ^* be replaced with the pipe radius, R^*. Following the similar procedure as for channel, we obtain the following relationship:

$$\begin{aligned} C_f = \ & \frac{16}{Re_b} + 16\int_0^1 2r\,\overline{u_r' u_z'}\,r dr \\ & -16\int_0^1 (r^2-1)\left(I_z'' + \frac{\partial p''}{\partial z} + \frac{\partial \overline{u_z}}{\partial t}\right) r dr\ . \end{aligned} \tag{14}$$

The weighting factor for the Reynolds stress is proportional to a square of the radial distance from the pipe axis.

For a plane boundary layer with zero mean streamwise pressure gradient, the starting point of derivation is Eq. (1) (with $-\overline{dp/dx} = 0$). The velocity is nondimensionalized by the free stream velocity, U_∞^*, and the boundary layer thickness, δ^* (e.g., 99 % thickness). The Reynolds number is defined as $Re_\delta = U_\infty^*\delta^*/\nu^*$. The following conditions may be assumed instead of the conditions (A) and (C) for channel and pipe flows:

(A$'$) constant free stream velocity,
(C$'$) $(\partial\overline{u}/\partial y) = 0$ at $y = 1$ (strictly speaking, this is an approximation).

In this case, the relation is obtained by directly applying the triple integration to Eq. (1) and it reads

$$\begin{aligned} C_f = \ & \frac{4(1-\delta_d)}{Re_\delta} + 2\int_0^1 2(1-y)(-\overline{u'v'})\ dy \\ & -2\int_0^1 (1-y)^2\left(\overline{I_x} + \frac{\partial\overline{u}}{\partial t}\right)\ dy\ , \end{aligned} \tag{15}$$

where δ_d denotes the displacement thickness normalized by δ^*. For a stationary laminar plane boundary layer, the first contribution is $4(1-\delta_d)/Re_\delta \simeq 2.6/Re_\delta$ and the third contribution can be computed as $0.7/Re_\delta$ by using the similar solution of Howarth[7]. The summation of these contributions is identical to the well-known relation: $C_f \simeq 3.3/Re_\delta$ $(= 0.66/\sqrt{Re_x})$.

The meaning of the first term in Eq. (15), however, is not clear as in the cases of Eqs. (11) and (14) because this term also depends on the mean velocity profile via δ_d. Note that, for channel and pipe flows, the resulting relationships are simpler because of the condition of constant flow rate (i.e., condition (A)) In channel and pipe flows, only conditions (A) and (B) are essential for the present analysis and it is easy to modify conditions (C) and (D). For example, for a fully-developed

TABLE I: Contribution of each term of Eq. (14) to C_f (pipe flow at $Re_b = 5300$, $y_d^{+u} \simeq 15$).

	Laminar (first term)	Turbulent (second term)	Total (C_f)
No control	3.02×10^{-3}	6.25×10^{-3}	9.27×10^{-3}
Controlled	3.02×10^{-3}	4.02×10^{-3}	7.04×10^{-3}

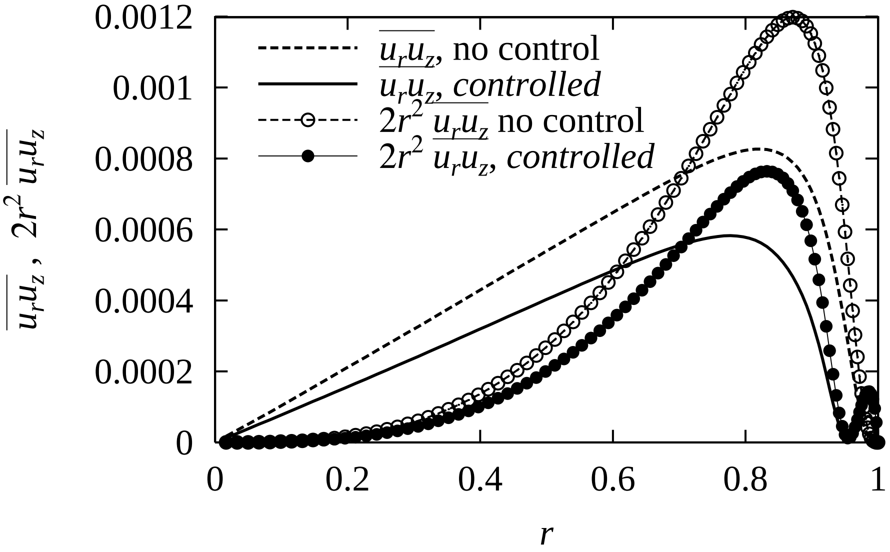

FIG. 2: Raw and weighted Reynolds stress distribution (nondimensionalized by R^* and $2U_b^*$) in uncontrolled and controlled pipe flows at $Re_b = 5300$ ($Re_{\tau u} \simeq 180$).

channel flow with uniform blowing and suction on the walls [8] (i.e., removal of condition (C)), the relation reads

$$\begin{aligned} C_f = \; & \frac{12}{Re_b} + 12\int_0^2 (1-y)(-\overline{u'v'})\,dy \\ & -12\,V_w \int_0^2 (1-y)\,\overline{u}\,dy\,, \end{aligned} \tag{16}$$

where V_w is the blowing/suction velocity at the walls and C_f is defined as an average of the friction coefficient on the two walls.

The advantage in the series of relations derived above is that one can quantitatively identify each dynamical contribution to the drag reduction/enhancement even for a manipulated flow. Here, we consider a fully developed turbulent pipe flow controlled by the opposition control algorithm[2], in which the third term of Eq. (14) is zero. The data were obtained by DNS based on the energy-conservative finite difference method [9] at the Reynolds number of $Re_b = 5300$ ($Re_{\tau u} \simeq 180$). The detection plane is set at $y_d^{+u} \simeq 15$. Here, a super- or subscript of u denotes a quantity nondimensionalized by the friction velocity of the uncontrolled flow. General results of this DNS are reported elsewhere[10], while we focus here on the derived relation.

Figure 2 shows the Reynolds stress, $\overline{u'_r u'_z}$, and the weighted Reynolds stress appearing in Eq. (14) (i.e., $2r^2\overline{u'_r u'_z}$). As is noticed in Eq. (14), the contribution of Reynolds stress near the wall is dominant both in uncontrolled and controlled cases. The difference in the areas covered by these two (controlled and uncontrolled) curves of the weighted Reynolds stress is directly proportional to the drag reduction by control. In the present case, the turbulent contribution is reduced by 35 %, though the total drag reduction is 24 % due to the presence of the laminar contribution as summarized in Table I. The contribution of Reynolds stress near the wall can be more clearly illustrated by plotting a cumulative contribution, $C_f^{T(cum)}$, to the turbulent part defined here as,

$$C_f^{T(cum)}(y) = 16\int_{1-y}^{1} 2r\overline{u'_r u'_z}\,rdr\,, \tag{17}$$

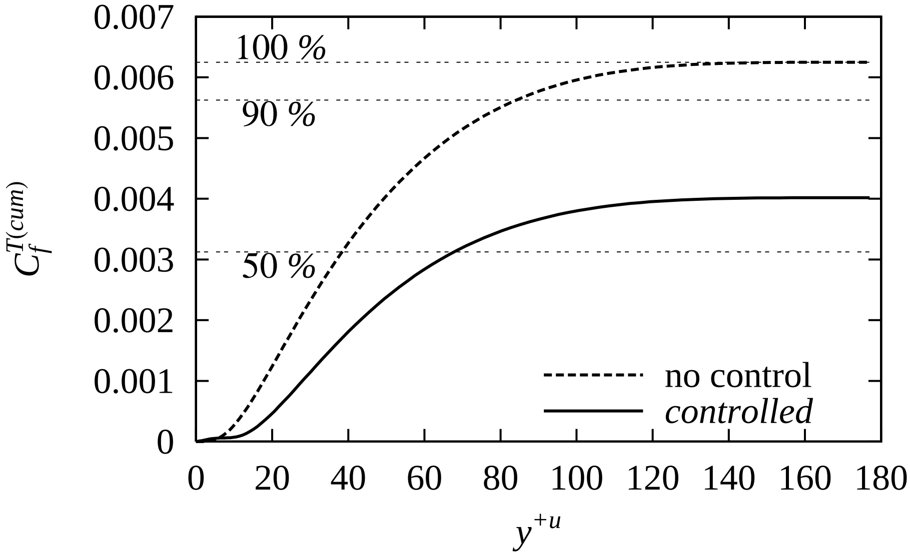

FIG. 3: Cumulative contribution of Reynolds stress (pipe flow, $Re_b = 5300$, $y_d^{+u} \simeq 15$).

where $y = (1 - r)$ is the distance from the wall. As is shown in Fig. 3, the Reynolds stress within 80 wall units from the wall is responsible for 90 % of the turbulent contribution to the skin friction in the case of uncontrolled flow. The opposition control algorithm by Choi *et al.*[2] utilizes this fact. Namely, it works to suppress the Reynolds stress near the wall, and results in considerable drag reduction in a low Reynolds number wall-bounded flow.

Another example is a fully-developed channel flow with uniform blowing on one wall and suction on the other. Table II and Fig. 4 show the componential contributions computed from the database[8] (`http://www.thtlab.t.u-tokyo.ac.jp/`), where the blowing/suction velocity is $V_w = V_w^*/(2U_b^*) = 0.00172$. For comparison, the case with $V_w = 0$ (an ordinary channel flow) at the same bulk Reynolds number ($Re_b \simeq 4360$) was also computed by the pseudospectral DNS code[11]. The turbulent contribution on the blowing side (defined here, for convenience, as $0 \leq y \leq 1$) is larger than that in the case of $V_w = 0$, while it is close to zero on the suction side ($1 \leq y \leq 2$). The total turbulent contribution is slightly reduced from the the ordinary channel flow. The convective contribution is negative on the blowing side and positive on the suction side. The total convective contribution is slightly positive. Since the total convective contribution exceeds the amount of reduction in the turbulent contribution, the total C_f results in a larger value than that of the ordinary channel flow.

In summary, we derived very simple, direct relationship between the Reynolds stress and the skin friction coefficient for three canonical wall-bounded turbulent flows, i.e., Eq. (11) for channel,

TABLE II: Contribution of each term of Eq. (16) to C_f (channel flow with/without uniform blowing/suction at $Re_b = 4357$, $V_w = 0.00172$).

	Laminar (first term)	Turbulent (second term)	Convective (Third term)	Total (C_f)
Without	2.8×10^{-3}	5.9×10^{-3}	0	8.7×10^{-3}
With	2.8×10^{-3}	5.6×10^{-3}	1.1×10^{-3}	9.5×10^{-3}

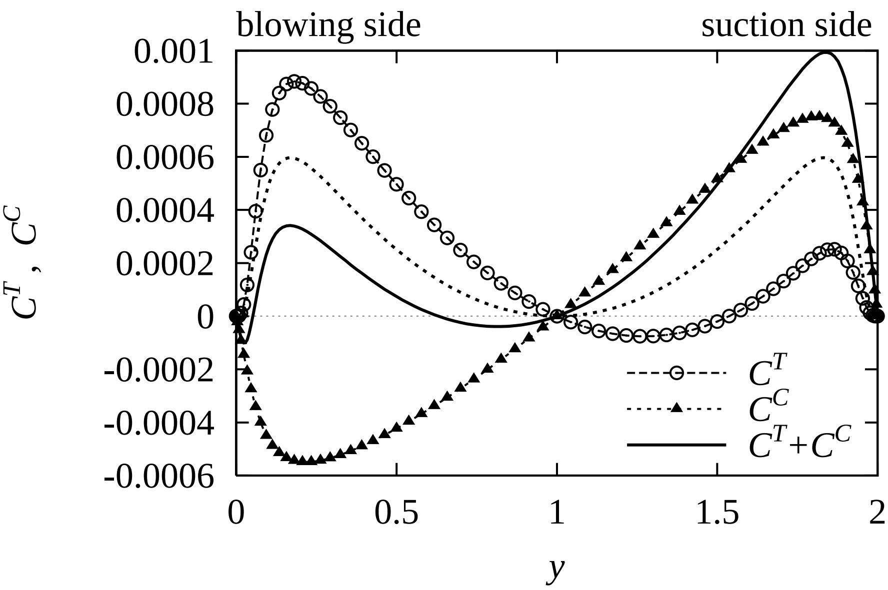

FIG. 4: Turbulent ($C^T = (1-y)(-\overline{u'v'})$) and convective ($C^C = -V_w(1-y)\overline{u}$) contributions in a channel flow with uniform blowing/suction ($Re_b \simeq 4360$, $V_w = 0.0017$). Dotted line is the turbulent contribution in an ordinary channel flow ($Re_b \simeq 4360$, $V_w = 0$).

Eq. (14) for pipe, Eq. (15) for plane boundary layer, respectively. Especially, for fully-developed turbulent channel and pipe flows, these relations reduce to

$$C_f = \frac{12}{Re_b} + 12 \int_0^1 2(1-y)(-\overline{u'v'})\, dy \tag{18}$$

and

$$C_f = \frac{16}{Re_b} + 16 \int_0^1 2r\, \overline{u_r' u_z'}\, rdr\, , \tag{19}$$

respectively. Usefulness of the relation was demonstrated through some examples of flow control. For drag reduction control, suppression of the Reynolds stress near the wall is of primary importance. It is also worth noting that turbulent skin friction becomes even smaller than that in laminar flow with a control algorithm which can make the turbulent part of Eqs. (11) and (14) negative. The present relationship enables quantitative discussion on the drag reduction/enhancement effects brought about by the modification of the flow structure, and may serve as a clue for development and evaluation of new control algorithms.

Acknowledgments

This work was supported through the Project for Organized Research Combination System by the Ministry of Education, Culture, Sports and Technology of Japan (MEXT).

---

[1] S. K. Robinson, “Coherent motions in the turbulent boundary layer,” Annu. Rev. Fluid Mech. **23**, 601 (1991).

[2] H. Choi, P. Moin, and J. Kim, “Active turbulence control for drag reduction in wall bounded flows,” J. Fluid Mech. **262**, 75 (1994).

[3] E. P. Hammond, T. R. Bewley, and P. Moin, “Observed mechanisms for turbulence attenuation and enhancement in opposition-controlled wall-bounded flows,” Phys. Fluids **10**, 2421 (1998).

[4] P. Koumoutsakos, “Vorticity flux control for a turbulent channel flow,” Phys. Fluids **11**, 248 (1999).

[5] T. Endo, N. Kasagi, and Y. Suzuki, “Feedback control of wall turbulence with wall deformation,” Int. J. Heat Fluid Flow **21**, 568 (2000).

[6] A. G. Kravchenko, H. Choi, and P. Moin, “On the relation of near-wall streamwise vortices to wall skin friction in turbulent boundary layers,” Phys. Fluids A **5**, 3307 (1993).

[7] L. Howarth, “On the solution of the laminar boundary layer equations,” Proc. Roy. Soc. London, Ser A **164**, 547 (1938).

[8] Y. Sumitani, and N. Kasagi, “Direct numerical simulation of turbulent transport with uniform wall injection and suction,” AIAA J., **33**, 1220 (1995).

[9] K. Fukagata and N. Kasagi, “Highly energy-conservative finite difference method for the cylindrical coordinate system,” J. Comput. Phys. **181** (2002) 478.

[10] K. Fukagata and N. Kasagi, “Active control for drag reduction in turbulent pipe flow,” in *Engineering Turbulence Modelling and Experiments - 5*, edited by W. Rodi and N. Fueyo (Elsevier Science, 2002) pp. 607-616.

[11] K. Iwamoto, Y. Suzuki, and N. Kasagi, “Reynolds number effect on wall turbulence: Toward effective feedback control,” Int. J. Heat Fluid Flow **23**, 678 (2002).